Inorganic Chemistry

Article

pubs.acs.org/IC

Two-Dimensional Coordination Polymers Constructed by [$Ni^{II}Ln^{III}$] Nodes and $[W^{IV}(bpy)(CN)_6]^{2-}$ Spacers: A Network of [$Ni^{II}Dy^{III}$] Single Molecule Magnets

Maria-Gabriela Alexandru,[†,‡] Diana Visinescu,[§] Sergiu Shova,[∥,⊥] Francesc Lloret,[#] Miguel Julve,*[,#] and Marius Andruh*[,†]

[†]Inorganic Chemistry Laboratory, Faculty of Chemistry, University of Bucharest, Str. Dumbrava Rosie 23, 020464 Bucharest, Romania

[‡]Department of Inorganic Chemistry, Physical Chemistry and Electrochemistry, Faculty of Applied Chemistry and Materials Science, University "Politehnica" of Bucharest, 1-7 Gh. Polizu Street, 011061 Bucharest, Romania

[§]Coordination and Supramolecular Chemistry Laboratory, "Ilie Murgulescu" Institute of Physical Chemistry, Romanian Academy, Splaiul Independentei 202, 060021 Bucharest, Romania

[∥]"Petru Poni" Institute of Macromolecular Chemistry of the Roumanian Academy, Aleea Grigore Ghica Vodă 41-A, RO-700487 Iasi, Romania

[⊥]Institute of Chemistry, Academy of Sciences of the Republic of Moldova, Str. Academiei 3, MD-2028 Chişinău, Moldavia

[#]Departament de Química Inorgànica/Instituto de Ciencia Molecular, Facultat de Química de la Universitat de València, C/Catedrático José Beltrán, 46980 Paterna, València, Spain

Supporting Information

ABSTRACT: Three isomorphous two-dimensional (2D) coordination polymers of general formula $\{[Ni^{II}(valpn)Ln^{III}(NO_3)(H_2O)(\mu\text{-}NC)_4W^{IV}(bipy)(CN)_2]\cdot xH_2O\cdot yCH_3CN\}_n$ have been synthesized by reacting $Ph_4P[W^V(CN)_6(bipy)]$ with the heterodinuclear $[Ni^{II}Ln^{III}(valpn)(O_2NO)_3]$ complexes [H_2valpn = 1,3-propanediyl-bis(2-iminomethylene-6-methoxyphenol), bipy = 2,2′-bipyridine, and Ln = Gd (**1**), Dy (**2**), and Tb (**3**) with x = 2 (**1**), 3.9 (**2**), and 3.35 (**3**) and y = 2.50 (**1**), 2 (**2**), and 1.8 (**3**)]. Their crystal structures consist of $[Ni^{II}Ln^{III}]$ 3d-4f nodes which are connected by $[W^{IV}(bipy)(CN)_6]^{2-}$ diamagnetic linkers resulting from the reduction of W^V to W^{IV} during the reaction process. The Ni(II) and Ln(III) ions occupy the inner and outer coordination sites of the dideprotonated valpn ligand, respectively, and they are doubly bridged by the phenoxo oxygen atoms of such a ligand. The value of Ni(II)···Ln(III) separation through this bridge is 3.4919(10) (**1**), 3.4760(10) (**2**), and 3.4799(9) (**3**) Å, and those of the angles at the bridgehead phenoxo atoms are 106.6(2) and 107.3(2) (**1**), 106.9(2), and 107.8(2) (**2**) and 106.5(2)−106.8(2)° (**3**). Each W(IV) is eight-coordinated with a bidentate bipy molecule and six cyanide-carbon atoms building a somewhat distorted square antiprism environment. The rare-earth cations are nine-coordinated, the donor atoms describing a monocapped square antiprism for **1** and **3** and a tricapped trigonal prism for **2**. Magnetic susceptibility measurements in the temperature range 1.9−300 K show the occurrence of ferromagnetic interactions between the Ni(II) and Ln(III) ions in **1**−**3**. Frequency-dependent alternating susceptibility signals were observed for the Dy^{III} derivative below 8.0 K under an applied dc field of 2500 G indicating the presence of slow magnetic relaxation with values of the pre-exponential factor (τ_0) and energy barrier ($E^{\#}$) of ca. 5.7×10^{-8} s and 15.9 cm^{-1}, respectively. Complex **2** constitutes the first example of a 2D 3d-4f heterobimetallic single molecule magnet (SMM).

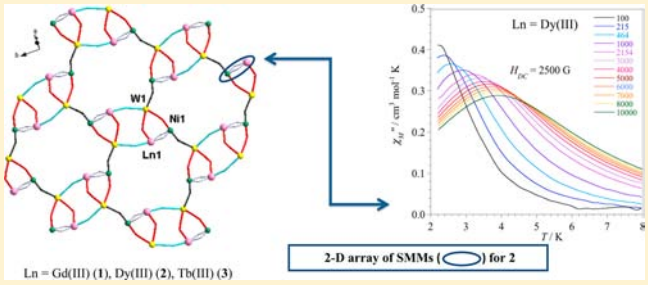

INTRODUCTION

Cyanido-complexes of transition d-block metals have provided well-known examples of building-blocks in the field of magnetochemistry, due to their stability and to the ability of the cyanide ligands to mediate strong magnetic interactions between d and d/f metal ions when acting as bridges. Homoleptic paramagnetic cyanido-metalloligands, such as $[Fe(CN)_6]^{3-}$, $[Cr(CN)_6]^{3-}$, $[Mo(CN)_8]^{3-}$, $[W(CN)_8]^{3-}$, are currently employed in designing nD heterobimetallic networks (n = 1−3) as well as heterotrimetallic assemblies.[1−10] The incorporation of the polydentate ancillary ligands in the coordination sphere of the metal ion causes a decrease of both the number of the cyanide groups and overall negative

Received: July 31, 2013
Published: September 25, 2013

charge of the cyanide-bearing unit, factors that in principle allow a better control of the dimensionality of the resulting products when used as ligands toward fully solvated metal ions of preformed species whose coordination sphere is coordinatively unsaturated. This is well illustrated by the precursors of formula $[M^{III}(AA)(CN)_4]^-$ [M = Fe and Cr; AA = 2,2′-bipyridine (bipy), 1,10-phenantroline (phen), or 2,2′-bipyrimidine (bpym)],[11] $[M^{III}(bpb)(CN)_2]^-$,[12] (bpb = 1,2-bis(pyridine-2-carboxamido)benzenate) or $[W^{V/IV}(bipy)(CN)_6]^{-/2-}$,[13] that usually lead to 1D coordination polymers or to oligonuclear complexes. Among the coordination networks obtained using a heteroleptic cyanido-complex, only a small number correspond to high-dimensional compounds: (i) a basket weave-like two-dimensional (2D) motif resulted from connecting Mn^{II} ions through the diamagnetic $[W^{IV}(bipy)(CN)_6]^{2-}$ anionic complex;[14] (ii) Pr^{III}–Fe^{III} and Fe^{II}–Ni^{II} 2D arrays were produced by using $[Fe^{III}(phen)(CN)_4]^-$ as a building block;[15] (iii) oxalato- and cyanido-bridged Cr^{III}–Mn^{II} complexes were synthesized from $[Cr^{III}(AA)(CN)_4]^-$ heteroleptic units, the oxalate being generated via oxidation–hydrolysis of diaminomalenitrile;[16] (iv) and 4d-4f and 3d-4d extended structures based on $[Ru^{III}(acac)_2(CN)_2]$[17] (Hacac = acetylacetone) and $[Ru^{II}(AA)(CN)_4]^{2-}$ tectons as ligands.[18]

The organization of single molecule magnets (SMMs) in crystals or on surfaces[19] is of great interest owing to the potential applications in data storage and molecular electronics. Several research groups have shown that the occurrence of weak magnetic interactions between SMMs, mediated by hydrogen bonds or bridging ligands, exert an influence on the quantum properties, shifting the quantum tunneling resonances with respect to the discrete SMMs.[20] Several examples of association of SMMs into well-defined nD coordinative and supramolecular architectures have been described recently.[20,21] The use of SMMs as nodes in constructing coordination polymers can lead to different magnetic materials, depending on the structural and electronic peculiarities of the spacers: (i) short spacers that favor relatively strong intramolecular ferro-/antiferromagnetic interactions transform the spin network into a classical ferro-/antiferromagnet; (ii) if the spacers are long enough and diamagnetic, the nodes preserve their SMM behavior; (iii) if the spacers themselves are paramagnetic, ferri- or ferromagnetic chains/single-chain magnets (SCMs) can be generated.[21]

Diamagnetic metallo-linkers, such as $[Co^{III}(CN)_6]^{3-}$, $[M^{IV}(CN)_8]^{4-}$ (M^{IV} = Mo and W), or organic molecules, could be employed to assemble extended structures of magnetically isolated SMM building-blocks.[21d−21k] Several examples of 2D and 3D frameworks constructed from SMM nodes are known, most of them being built from oxo-bridged Mn_x-based SMM motifs (x = 3, 4, 6, 19).[20a,21a−d] Only one example of high dimensional (2D) arrays of d-f heterometallic SMM units bridged by an organic molecule was described recently.[21g]

On the basis of the node and spacer approach to construct coordination polymers which was formulated by Robson in 1990[22] and having in mind the extension of this strategy using oligonuclear complexes as nodes and organic *exo*-dentate ligands or metalloligands as spacers,[23] we prepared three heterotrimetallic layered compounds containing $[Ni^{II}Ln^{III}]$ units [Ln = Gd (**1**), Dy (**2**), and Tb (**3**)] connected by $[W^{IV}(bipy)(CN)_6]^{2-}$ diamagnetic linkers. The Dy^{III} derivative was found to be a 2D network of SMMs. The synthesis, structural characterization and variable-temperature magnetic study of **1**−**3** are presented here.

EXPERIMENTAL SECTION

MATERIALS

The chemicals used as well as the solvents were of reagent grade, and they were purchased from commercial sources. The starting compounds $[Ni(valpn)(H_2O)_2]$ and $AsPh_4[W(bipy)(CN)_6]$ [H_2valpn = 1,3-propanediyl-bis(2-iminomethylene-6-methoxyphenol and $AsPh_4^+$ = tetraphenylarsonium cation] were synthesized by following the literature procedures.[24,25]

Synthesis of $\{[Ni^{II}(valpn)Ln^{III}(NO_3)(H_2O)(\mu\text{-}NC)_4W^{IV}(bipy)(CN)_2]\cdot xH_2O\cdot yCH_3CN\}_n$ [Ln = Gd (1), Dy (2), and Tb (3)]. All compounds were synthesized following the same general procedure: a solution of $AsPh_4[W(bipy)(CN)_6]$ (17 mg, 0.02 mmol) in acetonitrile (10 cm^3) was poured slowly into an acetonitrile solution (10 cm^3) containing $[Ni(valpn)(H_2O)_2]$ (8 mg, 0.02 mmol) and the corresponding hydrated lanthanide nitrate (0.02 mmol). The resulting violet solution was left undisturbed for two weeks. X-ray quality violet plate-like crystals were obtained. Yield: ca. 55 (**1**), 63 (**2**) and 47% (**3**). Anal. Calcd for $C_{40}H_{41.50}GdN_{13.50}NiO_{10}W$ (**1**): C, 37.76; H, 3.26; N, 14.86. Found: C, 37.45; H, 3.21; N, 14.79%. Anal. Calcd for $C_{39}H_{43.8}DyN_{13}NiO_{11.9}W$ (**2**): C, 36.27; H, 3.39; N, 14.10. Found: C, 36.22; H, 3.33; N, 14.07%. Anal. Calcd for $C_{38.6}H_{42.10}TbN_{12.80}NiO_{11.35}W$ (**3**): C, 36.51; H, 3.32; N, 14.12. Found: C, 37.32; H, 3.28; N, 14.09%. Ni:Ln molar ratio (electron probe X-ray microanalysis): 1:1 for **1**−**3**. IR (KBr, cm^{-1}): 3340m, ν(C≡N): 2120s, ν(C═N): 1635m, 1607m, 1473s, $\nu(NO_3)$: 1384vs, 1304m, 1223s, 1073m, 742m (**1**); 3430s, ν(C≡N): 2120s, ν(C═N): 1634s, 1608m, 1470s, $\nu(NO_3)$: 1384m, 1300m, 1220m, 1070m, 740m (**2**); 3320m, ν(C≡N): 2120s, ν(C═N): 1634s, 1607m, 1470s, $\nu(NO_3)$: 1384vs, 1301s, 1223 1070m, 742m (**3**).

Physical Measurements. Elemental analyses (C, H, N) were performed with a Perkin-Elmer 2400 analyzer. The Ni/Ln molar ratio was determined through electron probe X-ray microanalysis by using a Philips XL-30 scanning electron microscope (SEM) from the Central Service for Support to Experimental Reseach (SCSIE) at the University of València. IR spectra were recorded with a FTIR Bruker Tensor V-37 spectrophotometer using KBr pellets in the range 4000−400 cm^{-1}. Direct current (dc) magnetic susceptibility measurements on crushed crystals of **1**−**3** (mixed with grease to avoid the crystallite orientation) were carried out with a Quantum Design MPMSXL-5 SQUID magnetometer in the temperature range 1.9−300 K and under applied dc magnetic fields of 5000 G ($T \geq 50$ K) and 100 G ($1.9 \leq T \leq 50$ K). Magnetization versus H field measurements were done at 2.0 K in the field range 0−5 T. Alternating current (ac) magnetic susceptibility measurements were recorded at low temperatures (2.1−8.0 K) under different dc static fields (0−5000 G) and ±54 G oscillating field at frequencies in the range 100−10000 Hz. The magnetic susceptibility data were corrected for the diamagnetism of the constituent atoms and the sample holder.

X-ray Data Collection and Structure Refinement. X-ray data for single crystals of **1**−**3** with dimensions 0.20 × 0.20 × 0.05 (**1**), 0.10 × 0.10 × 0.05 (**2**), and 0.15 × 0.15 × 0.04 mm (**3**) were carried out with an Oxford Diffraction XCALIBUR E CCD diffractometer equipped with graphite-monochromated Mo Kα radiation (l = 0.71073 Å). The crystals were placed 40

dx.doi.org/10.1021/ic4019794 | *Inorg. Chem.* 2013, 52, 11627−11637

Table 1. Crystallographic Data for 1, 2, and 3

	1	2	3
chemical formula	$C_{40}H_{41.5}NiWN_{13.5}O_{10}Gd$	$C_{39}H_{43.8}NiWN_{13}O_{11.9}Dy$	$C_{38.6}H_{42.1}NiWN_{12.8}O_{11.35}Tb$
formula weight	1271.18	1290.13	1268.43
T, K	100.00(10)	100.00(10)	99.9(2)
wavelength, Å	0.71073	0.71073	0.71073
crystal system, space group	monoclinic $P2_1/n$	monoclinic $P2_1/n$	monoclinic $P2_1/n$
unit cell dimensions			
a, Å	14.4542(7)	14.4382(4)	14.4585(9)
b, Å	22.6068(7)	22.5081(6)	22.5407(11)
c, Å	15.7197(8)	15.7160(5)	15.7106(10)
α, °	90	90	90
β, °	111.966(6)	111.866(4)	111.913(8)
γ, °	90	90	90
V, Å^3	4763.7(4)	4739.9(9)	4750.3(5)
Z	4	4	4
calculated density, g/cm^3	1.772	1.808	1.774
absorption coefficient, mm^{-1}	4.244	4.446	4.350
F(000)	2488	2528	2484
crystal dimensions, mm	0.2 × 0.2 × 0.05	0.1 × 0.1 × 0.05	0.15 × 0.15 × 0.04
2θ range for data collection, °	4.72−52	4.72−52	4.84−52
reflections collected	24284	28412	28334
independent reflections	9319 [R(int) = 0.0562]	9298[R(int) = 0.0800]	[R(int) = 0.0646]
data/restraints/parameters	9319/3/597	9298/70/607	9288/39/595
goodness-of-fit on F	1.011	1.027	1.039
final R indices [$I > 2\sigma(I)$]	R_1 = 0.0504; wR_2 = 0.1049	R_1 = 0.0532; wR_2 = 0.0871	R_1 = 0.0457; wR_2 = 0.0938
R indices (all data)	R_1 = 0.0728; wR_2 = 0.1140	R_1 = 0.0830; wR_2 = 0.0955	R_1 = 0.0657; wR_2 = 0.1011
refinement method	full-matrix least-squares on F^2		

Table 2. Selected Bond Lengths [Å], Contact Distances [Å], and Bond Angles [°] for 1[a]

	1		1		1		1		1
Ni1−N7$_{ax}$	2.124(6)	Gd1−O1	2.304(5)	Gd1···W1	5.3193(6)	C29−N6−Gd1	137.7(6)	Ni1−O1−Gd1	106.6(2)
Ni−N9$_{ax}$	2.069(6)	Gd1−O2	2.301(5)	Ni1···W1	5.1189(9)	C30−N7−Ni1	141.3(6)	Ni1−O2−Gd1	107.3(2)
Gd1−N6	2.490(6)	Gd1−O3	2.514(5)	Gd1···Ni1	3.4919(10)	C31−N8−Gd1a	161.1(5)	O2−Ni1−N7	87.2(2)
Gd1−N8	2.489(6)	Gd1−O4	2.516(5)	Gd1a···W1	5.6790(5)	C32−N9−Ni1b	154.1(6)	O2−Ni1−N2	91.8(2)
W1−C29	2.149(7)	Gd1−O5	2.544(5)	Ni1b···W1	5.2152(9)			O2−Ni1−N9	90.5(2)
W1−C30	2.145(7)	Gd1−O6	2.496(5)			O1W−Gd1−O2	109.65(16)	O2−Ni1−N12	168.0(2)
W1−C31	2.119(7)	Gd1−O1W	2.497(5)	N6−C29−W1	174.2(6)	O1−Gd1−O2	67.38(17)	O2−Ni1−O1	77.6(2)
W1−C32	2.135(8)	Ni1−N2	2.042(7)	N7−C30−W1	176.0(6)	O2−Gd1−O3	129.32(17)	N2−Ni1−N7	86.6(2)
W1−C33	2.156(8)	Ni1−N12	2.038(6)	N8−C31−W1	179.0(7)	O1W−Gd1−O3	71.76(17)	N2−Ni1−N9	86.2(2)
W1−C34	2.171(8)	Ni1−O1	2.047(5)	N9−C32−W1	178.1(6)	O1W−Gd1−O4	140.13(16)	N12−Ni1−O1	90.5(2)
W1−N4	2.205(6)	Ni1−O2	2.031(5)			O1W−Gd1−N8	75.99(19)	N12−Ni1−N9	89.8(2)
W1−N5	2.223(6)					O1W−Gd1−O1	74.08(17)	N4−W1−N5	72.4(2)

[a] a = 1 − x, 1 − y, −z; b = −0.5 +x, 0.5 −y, −0.5 + z.

Table 3. Selected Bond Lengths [Å], Contact Distances [Å], and Bond Angles [°] for 2[a]

	2		2		2		2		
Ni1−N6$_{ax}$	2.083(6)	Dy1−O1	2.274(5)	Dy1···W1	5.3175(5)	C30−N6−Ni1b	154.0(6)	Ni1−O1−Dy1	107.75(19)
Ni−N7$_{ax}$	2.138(6)	Dy1−O2	2.281(5)	Ni1···W1	5.1199(9)	C31−N7−Ni1	141.6(6)	Ni1−O2−Dy1	106.86(19)
Dy1−N8	2.459(6)	Dy1−O3	2.502(5)	Dy1···Ni1	3.4760(10)	C32−N8−Dy1	138.8(6)	O2−Ni1−N7	93.5(2)
Dy1−N10	2.429(6)	Dy1−O4	2.479(5)	Dy1a···W1	5.6463(5)	C34−N10−Dy1a	162.7(6)	O2−Ni1−N2	91.0(2)
W1−C30	2.144(8)	Dy1−O5	2.467(5)	Ni1b···W1	5.2178(10)	O1W−Dy1−O2	74.56(15)	O2−Ni1−N6	93.4(2)
W1−C31	2.150(7)	Dy1−O6	2.506(5)			O1−Dy1−O2	67.64(16)	O2−Ni1−N1	169.3(2)
W1−C32	2.147(7)	Dy1−O1W	2.484(5)	N6−C30−W1	178.2(7)	O2−Dy1−O3	128.48(15)	O2−Ni1−O1	76.76(18)
W1−C33	2.164(8)	Ni1−N2	2.031(6)	N7−C31−W1	175.6(7)	O1W−Dy1−O3	140.06(15)	N2−Ni1−N7	94.2(2)
W1−C34	2.139(8)	Ni1−N1	2.027(6)	N8−C32−W1	173.2(6)	O1W−Dy1−O4	71.48(17)	N2−Ni1−N6	89.8(2)
W1−C35	2.185(7)	Ni1−O1	2.026(5)	N10−C34−W1	179.3(7)	O1W−Dy1−N8	69.51(17)	N1−Ni1−O1	92.6(2)
W1−N4	2.218(6)	Ni1−O2	2.043(5)	N9−C33−W1	175.2(7)	O1W−Dy1−O1	109.88(16)	N1−Ni1−N6	86.7(2)
W1−N5	2.218(6)			N11−C35−W1	173.5(7)			N4−W1−N5	72.0(2)

[a] a = −x, 1 − y, 1 − z; b = −0.5 + x, 1.5 − y, −0.5 + z.

dx.doi.org/10.1021/ic4019794 | Inorg. Chem. 2013, 52, 11627−11637

Table 4. Selected Bond Lengths [Å], Contact Distances [Å], and Bond Angles [°] for 3[a]

	2				2		2		
Ni1−N6$_{ax}$	2.082(5)	Tb1−O1	2.299(4)	Tb1···W1	5.3199(6)	C30−N6−Ni1b	154.0(5)	Ni1−O1−Tb1	106.82(19)
Ni−N7$_{ax}$	2.130(5)	Tb1−O2	2.296(4)	Ni1···W1	5.1189(9)	C31−N7−Ni1	141.7(5)	Ni1−O2−Tb1	106.5(2)
Tb1−N8	2.479(5)	Tb1−O3	2.518(5)	Tb1···Ni1	3.4799(9)	C32−N8−Tb1	138.4(5)	O2−Ni1−N7	93.48(19)
Tb1−N10	2.440(6)	Tb1−O4	2.504(5)	Tb1a···W1	5.6588(2)	C34−N10−Tb1a	162.6(5)	O2−Ni1−N2	90.6(2)
W1−C30	2.129(7)	Tb1−O5	2.485(5)	Ni1b···W1	5.2185(9)	O1W−Tb1−O2	74.43(17)	O2−Ni1−N6	93.5(2)
W1−C31	2.165(7)	Tb1−O6	2.518(5)			O1−Dy1−O2	67.37(16)	O2−Ni1−N1	169.3(2)
W1−C32	2.137(7)	Tb1−O1W	2.491(4)	N6−C30−W1	178.5(6)	O2−Tb1−O3	128.53(17)	O2−Ni1−O1	77.72(18)
W1−C33	2.178(7)	Ni1−N2	2.028(6)	N7−C31−W1	176.0(6)	O1W−Tb1−O3	140.00(17)	N2−Ni1−N7	94.4(2)
W1−C34	2.122(7)	Ni1−N1	2.041(6)	N8−C32−W1	173.5(6)	O1W−Tb1−O4	71.18(16)	N2−Ni1−N6	89.6(2)
W1−C35	2.178(7)	Ni1−O1	2.031(4)	N10−C34−W1	178.7(6)	O1W−Tb1−N8	69.83(16)	N1−Ni1−O1	91.6(2)
W1−N4	2.222(5)	Ni1−O2	2.044(5)	N9−C33−W1	174.9(6)	O1W−Tb1−O1	110.41(15)	N1−Ni1−N6	86.4(2)
W1−N5	2.219(5)			N11−C35−W1	173.0(6)			N4−W1−N5	72.1(2)

[a] $a = 2 - x, 1 - y, 1 - z$; $b = 0.5 + x, 1.5 - y, 0.5 + z$.

mm from the CCD detector. The unit-cell determination and data integration were carried out using the CrysAlis package of Oxford Diffraction.[26] All structures were solved by direct methods using SHELXS-97[27] and refined by full-matrix least-squares on F_o^2 with SHELXL-97[27] with anisotropic displacement parameters for the non-hydrogen atoms. All hydrogen atoms attached to carbon were introduced in idealized positions (d_{C-H} = 0.96 Å) using the riding model with their isotropic displacement parameters fixed at 120% of their riding atom. Positional parameters of the hydrogen atoms of the water molecules were obtained from difference Fourier syntheses and verified by the geometric parameters of the corresponding hydrogen bonds. The unit cell parameters and refinements conditions are given in Table 1 (**1**−**3**), whereas selected bond lengths and angles are listed in Tables 2 (**1**), 3 (**2**), and and 4 (**3**).

RESULTS AND DISCUSSION

Synthesis and IR Characterization. Three coordination polymers of general formula $[Ni^{II}(valpn)Ln^{III}(NO_3)(H_2O)(\mu\text{-}NC)_4W^{IV}(bipy)(CN)_2]_n$ [Ln = Gd (**1**), Dy (**2**), and Tb (**3**); H_2valpn is the Schiff-base resulting from the condensation of *o*-vanillin with 1,3-diaminopropane] were produced by a one-step reaction of the mononuclear $AsPh_4[W^V(bipy)CN)_6]$ species with the dinuclear $[Ni(valpn)Ln(O_2NO)_3]$ complexes. In a previous report, we presented the first heterotrimetallic complexes which are obtained using $[W^V(bipy)(CN)_6]^-$ as a metalloligand.[13d] The discrete heterotrimetallic compounds were obtained from the reaction of $[W^V(bipy)(CN)_6]^-$ with $[Cu^{II}Ln^{III}]$ complexes. Interestingly, when reacting the same building-block with very similar 3d-4f cationic species ($[Ni^{II}Ln^{III}]$ instead of $[Cu^{II}Ln^{III}]$ dinuclear complexes), W(V) was reduced to W(IV) ($[W^{IV}(bipy)(CN)_6]^{2-}$). This monoelectronic reduction of W(V) to W(IV) during the assembly process is not uncommon. Several authors reported the redox instability of the cyanido-complex $[W^V(CN)_8]^{3-}$, which in reaction with fully solvated metal ions or preformed metal complexes generates coordination networks containing W(IV).[28]

The presence of $[W^{IV}(bipy)(CN)_6]^{2-}$ within the three 2D networks is confirmed by the IR spectra, showing the stretching band of the cyanido groups at 2118 cm^{-1}, a value that is characteristic for a tungsten(IV) cyanido-complex.[25] In order to check whether the same 2D networks will result, and based on this observation, we carried out the synthesis using $[W^{IV}(bipy)(CN)_6]^{2-}$ as precursor. We could not obtain X-ray quality crystals, but the comparison of the FTIR spectra of the resulting powdered samples with those of the corresponding complexes **1**−**3** suggests that different compounds were obtained: in the case of the 2D coordination polymers **1**−**3**, the FTIR spectra display very strong peaks at 1384 cm^{-1}, which are assigned to the stretching vibration of the nitrate anion. These peaks are absent in the other cases, that is, when the reactant was $[W^{IV}(bipy)(CN)_6]^{2-}$. This indicates that the stoichiometry of the compounds obtained starting from the W(IV) derivative is different from those resulting by using $[W^V(bipy)(CN)_6]^-$ as the cyanide-bearing species.

Description of the Structures. Compounds **1**−**3** crystallize in the monoclinic system, space group $P2_1/n$. Since these complexes are isomorphous, only the structure of **1** will be discussed in detail hereafter, and we will refer to the other two when needed.

The structure of **1** consists of a neutral 2D motif of formula $[Ni^{II}(valpn)Gd^{III}(NO_3)(H_2O)(NC)_4W^{IV}(bipy)(CN)_2]_n$ plus crystallization acetonitrile and water molecules. The layered network contains heterotrimetallic $\{Ni^{II}Gd^{III}W^{IV}\}$ units (see Figure 1; Figures S1 and S2, Supporting Information for **2** and **3**, respectively), that comprise the diphenoxo-bridged $\{Ni^{II}Gd^{III}\}$ dinuclear nodes and the $[W^{IV}(bipy)(CN)_6]^{2-}$ spacers which coordinate to both Ni^{II} and Gd^{III} belonging to the same binuclear node and to one Ni^{II} and one Gd^{III} centers from two other nodes through four of their six cyanide groups.

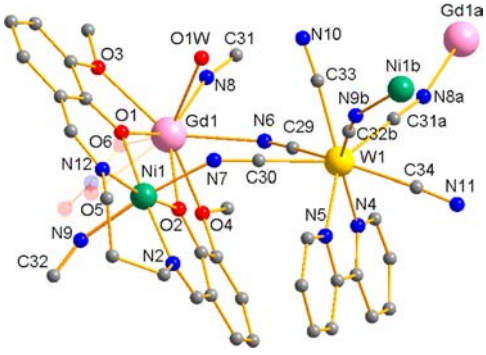

Figure 1. A view of the asymmetric unit of **1** along with the atom numbering scheme (the solvent molecules are omitted for clarity).

The tungsten(IV) ion is eight-coordinated by two nitrogen atoms from a bidentate bipy ligand and six cyanide-carbon atoms building a distorted square antiprism environment

dx.doi.org/10.1021/ic4019794 | Inorg. Chem. 2013, 52, 11627−11637

[Figure 2 (**1**) and S3a (**2**) and S3b (**3**)]. The value of the normalized bite angles for the chelating bipy is 1.18 in **1**–**3**,[29]

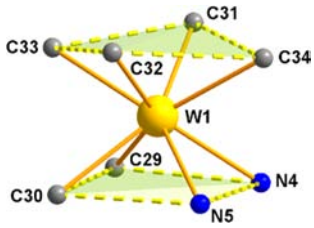

Figure 2. A view of the environment of the W(IV) ion in **1** showing only the coordinating atoms.

and those of the dihedral angle between the upper and basal mean planes are 1.43 (**1**), 1.36 (**2**), and 2.11° (**3**). The W–C bond lengths in **1** vary in the range 2.119(7)–2.171(8) Å [2.139(8)–2.185(7) (**2**) and 2.122(7)–2.178(7) Å (**3**)], values that are somewhat shorter than those of W–N [2.205(6) and 2.223(6) (**1**), 2.218(6) (**2**) and 2.219(5) and 2.222(5) Å (**3**)].

The nickel(II) ion in **1** exhibits a slightly distorted octahedral coordination geometry, with the equatorial positions occupied by two nitrogen and two phenoxo oxygen atoms arising from the inner compartment of the Schiff-base ligand [Ni1–N2 = 2.042(7), Ni1–N12 = 2.038(6), Ni1–O1 = 2.047(5), and Ni1–O2 = 2.031(5) Å (**1**)], whereas the axial positions are filled by two cyanido bridging groups from the cyanide-tungstate linkers [Ni1–N7 = 2.1235(51) and Ni1–N9 = 2.0679(53) Å]. The same donor set occurs for the nickel(II) ion in **2** and **3** with very close values for the bond lengths (see Tables 3 and 4). The values of the distance between the Ni(II) and Ln(III) ions through the diphenoxo bridges are 3.4919(10) (**1**), 3.4760(10) (**2**), and 3.4799(9) Å (**3**), and the angles involving the bridgehead phenoxo atoms are 106.6(2) and 107.3(2) (**1**), 106.9(2) and 107.8(2) (**2**), and 106.5(2)–106.8(2)° (**3**). The values of the hinge angle (dihedral angle between the O–Ni–O and O–Ln–O planes) are equal to 10.07 (**1**), 10.32 (**2**), and 10.74° (**3**). The bond lengths and angles related to the $\{Ni^{II}Gd^{III}\}$ moiety are in agreement with previous reports on parent systems.[24,30]

Each Gd(III) ion is nine-coordinated by two nitrogen atoms from two cyanido bridges and seven oxygen atoms, four of them from the valpn ligand, two from a bidentate nitrato, and the remaining one from a water molecule. Concerning the coordination environment for the Gd(III) ion, the best description would be a distorted monocapped square antiprism, the capping position being occupied by an oxygen atom (O6) belonging to the nitrato ligand [see Figure 3 (left)]. The torsion angle of the upper square plane N8–O4–O5–O3 is 18.7°, while the lower square base formed by the atoms OW1–N6–O2–O1 is closer to planarity (torsion angle ca. 3.7°).

The Tb(III) environment in **3** is also nine-coordinated in a distorted monocapped square antiprism like the Gd(III) ion in **1** [see Figure 3 (right)] with the values of the structural parameters being very close. However, the Dy(III) ion in **2** displays a tricapped trigonal prism coordination geometry [see Figure 3 (middle)]. The three capping positions are filled by the N8 atom from a bridging cyanide and the O5 and O2 oxygen atoms from the bidentate nitrato ligand and the phenoxo bridge, respectively. The angles between the adjacent bonds formed by the capping atoms (O2, N8, and O5) and the Dy(III) cation are close to the ideal value of 120°, and the four atoms are quasi coplanar (torsion angle of 5.5°).

The heterometallic structure in **1** (the same applies for compounds **2** and **3**) is expanded into a quite interesting 2D network as follows: a trinuclear unit {Ni1Gd1W1} [red fragment in Figure 4; Figures S4 (**2**) and S5 (**3**)] is connected to another trinuclear unit through two cyanido groups [sky blue in Figure 4; Figures S4 (**2**) and S5 (**3**)] and leads to a hexanuclear $\{(NiGdW)_2(\mu\text{-}CN)_2\}$ moiety; each hexanuclear moiety is further connected to four other hexanuclear fragments through cyanido bridges [black in Figure 4; Figures S4 (**2**) and S5 (**3**)]. The Ni1···W1 and Gd1···W1 distances across the cyanido bridges within a trimetallic unit are equal with 5.1189(9) and 5.3193(6) Å, respectively [138.8(6) and 141.6(6)° for **2**; 138.4(5) and 141.7(5)° for **3**]. The tungsten(IV) and gadolinium(III) ions from two different trinuclear units which form the hexanuclear fragments are spaced across the cyanido bridges by 5.3193(6) Å [W1···Gd1a contact with (a) = $1 - x$, $1 - y$, $-z$] [5.6463(5) Å for W1···Dy1a with (a) = $-x$, $1 - y$, $1 - z$ and 5.6588(5) Å for W1···Tb1a with (a) = $2 - x$, $1 - y$, $1 - z$]. The distance between W^{IV} and Ni^{II} metal ions, belonging to two hexanuclear units, connected by cyanido ligands is 5.2152(9) Å [W1···Ni1b with (b) = $-0.5 + x$, $0.5 - y$, $-0.5 + z$] [5.2178(10) Å, (b) = $-0.5 + x$, $1.5 - y$, $-0.5 + z$ for **2** and 5.2185(9) Å, (b) = $0.5 + x$, $1.5 - y$, $0.5 + z$ for **3**].

The packing of the neutral layers in **1** generates star-shaped channels along the crystallographic *a* axis (see Figure 5). Similar channels are also observed when changing the viewing direction along the *c* axis. The cavities are described by 28-membered metallacycles, and they are large enough to confine the solvent molecules (acetonitrile and water). The distances between diagonally positioned metal ions belonging to the same metallacycle are 12.54 (Ni···Ni), 11.50 (Gd···Gd) and 15.46 Å (W···W) [12.49 (Ni···Ni), 11.51 (Dy···Dy) and 15.44 Å (W···W) for **2**, and 12.50 (Ni···Ni), 11.52 (Tb···Tb) and 15.44 Å (W···W) for **3**]. Thereby, the structure can be considered a porous framework that comprises the heteroleptic

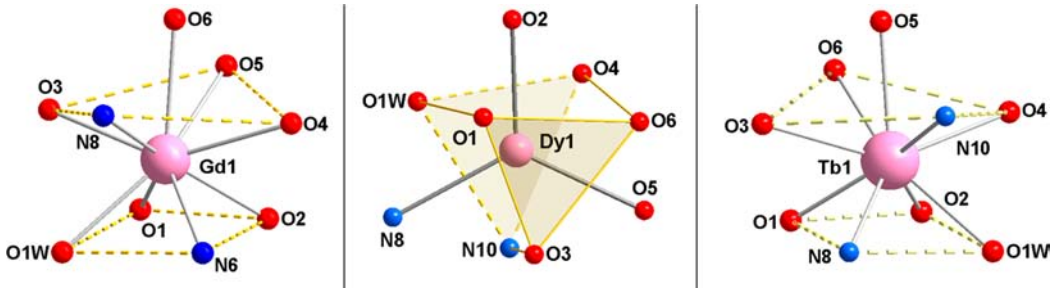

Figure 3. Coordination polyhedra of the Gd(III), Dy(III), Tb(III) in the compounds **1**, **2**, and **3**, respectively.

dx.doi.org/10.1021/ic4019794 | *Inorg. Chem.* 2013, 52, 11627–11637

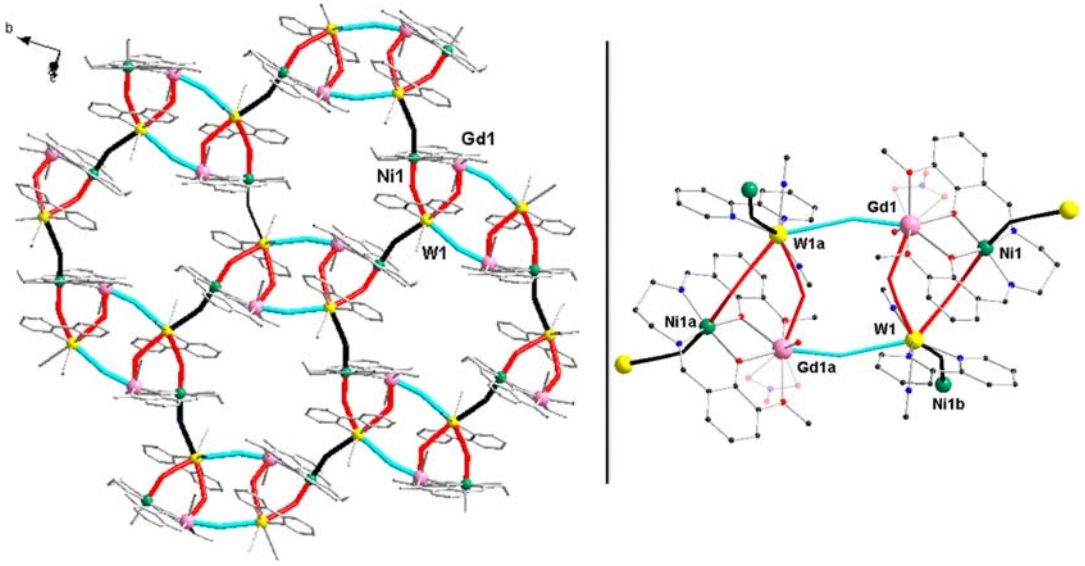

Figure 4. (Right) View of a fragment of the 2D structure of **1**. (Left) Detail showing a hexanuclear unit. The solvent molecules of crystallization and the H-atoms are omitted for clarity.

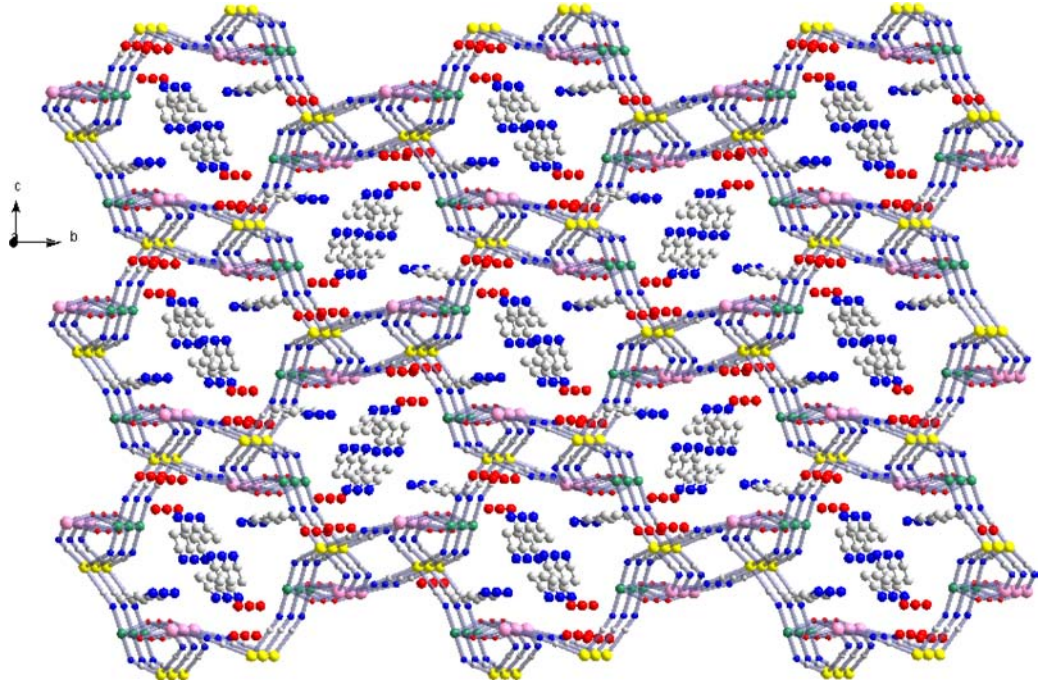

Figure 5. A View of the packing of **1** along the crystallographic *a* axis showing the porous nature of the framework and the solvent filling (acetonitrile – gray/blue ball and stick and water molecules – red spheres).

tetradentate metalloligand spacer $[W^{IV}(bipy)(CN)_4]^{2-}$ and the heterobimetallic node $[Ni^{II}(valpn)Gd^{III}(O_2NO)_3]^{2+}$. It is worth mentioning the high denticity of the $[W^{IV}(bipy)(CN)_6]^{2-}$ cyanide complex. The structure expands into a 2D network due to the tetradentate coordinating metalloligand. The heteroleptic unit was found to be a mono-, bi-, and tridentate metalloligand in three structures reported to date that contain this motif.[13e,14]

Hydrogen bonds between the solvent molecules and the terminal cyanido ligands afford supramolecular chains in **1** (see Figure 6) and connect the neutral layers leading to a supramolecular 3D network. The crystallization water molecules O2W and O3W, the coordinated water OW1 and the nitrogen atom N10 belonging to a terminal cyanide ligand are connected through hydrogen bonds and lead to an interesting supramolecular heteronuclear distorted square. The donor–acceptor distances involving the hydrogen bonds are in the 2.64–3.12 Å range for **1** (see Table S1).

Magnetic Properties. The magnetic properties of **1** under the form of the $\chi_M T$ against T plot [χ_M if the magnetic susceptibility per Ni(II)Gd(III)unit] are shown in Figure 7. At room temperature, $\chi_M T$ is equal to 9.10 $cm^3\ mol^{-1}\ K$, a value that is compatible with the calculated value for a magnetically noninteracting Ni(II)Gd(III) couple [$\chi_M T$ = 8.98 $cm^3\ mol^{-1}\ K$ with S_{Ni} = 1, S_{Gd} = 7/2, g_{Ni} = 2.10 and g_{Gd} = 2.0]. The $\chi_M T$ product increases continuously with decreasing temperature to

dx.doi.org/10.1021/ic4019794 | *Inorg. Chem.* 2013, 52, 11627–11637

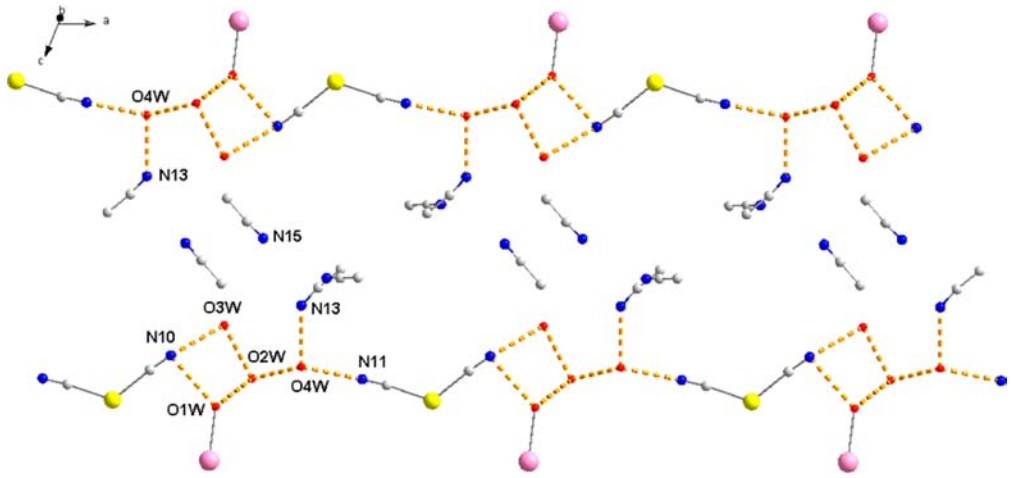

Figure 6. A view of the supramolecular chains through hydrogen bonds growing parallel to the crystallographic *b* axis.

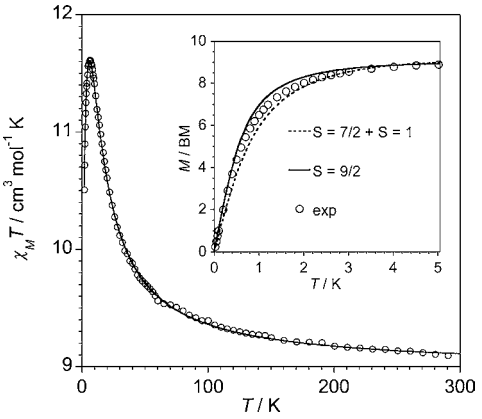

Figure 7. Thermal dependence of $\chi_M T$ for **1**: (○) experimental data, (—) best-fit curve through eq 1 (see text). The inset shows the field dependence of the magnetization at 2.0 K: (○) experimental data; (--) theoretical curve for isolated Ni(II) and Gd(III) ions; (—) theoretical line for an $S = 9/2$ with $g = 2.0$). The plots of the inset are referred to respectively as (a), (b), and (c) in the text.

reach a maximum value of 11.63 $cm^3\ mol^{-1}$ K at 6.0 K and then shows a sharp decrease down 2.0 K to a value of 10.50 $cm^3\ mol^{-1}$ K. The profile of the curve indicates that the Gd(III) and the Ni(II) interact ferromagnetically, leading to a $S = 9/2$ ground state, the decrease of $\chi_M T$ at very low temperatures being due to the zero-field splitting effects and/or interdimer antiferromagnetic interactions. The ferromagnetic interactions are further supported by the field dependence of the magnetization (M) at 2.0 K (see inset of Figure 7). One can see therein a comparison of the experimental values of M with the sum of the Brillouin functions for isolated Gd(III) ($S_{Gd} = 7/2$) and Ni(II) ($S_{Ni} = 1$) ions and the Brillouin function for an $S = 9/2$ pair state. The experimental values of M are somewhat above those of the magnetically isolated Gd(III)−Ni(II) pair and very close to those of $S = 9/2$. The slight difference between (a) and (c) is mainly due to the zero-field splitting effects.

Having in mind the diphenoxo-bridged Ni(II)Gd(III) dinuclear unit, the magnetic susceptibility data of **1** were analyzed by using the following spin Hamiltonian (eq 1)

$$\mathbf{H} = -J\mathbf{S}_{Gd}\cdot\mathbf{S}_{Ni} + D_{Ni}(\mathbf{S}^2_{zNi} + 2/3) + \beta\mathrm{H}(g_{Gd}\mathbf{S}_{Gd} + g_{Ni}\mathbf{S}_{Ni}) \quad (1)$$

where the first term deals with the isotropic interaction (J is the magnetic coupling across the double phenoxo bridge), the second one corresponds to the local anisotropy of the octahedral nickel(II) ion, and the last one is the Zeeman interaction. With the lack of an analytical expression to treat the magnetic data of **1**, we tried to model them through numerical matrix diagonalization techniques using a Fortran program[31] (conducting extensive mapping with the aim of locating the global minimum of each system along a large amount of local minima). The set of best-fit parameters are $J = +2.57\ cm^{-1}$, $|D_{Ni}| = 4.89\ cm^{-1}$, $g_{Ni} = 2.12$, $g_{Gd} = 2.0$, $\theta = -0.35$ K, and $R = 1.3 \times 10^{-5}$ (R is the agreement factor defined as $\sum_i[(\chi_M T)_{exp}(i) - (\chi_M T)_{calc}(i)]/\sum_i[(\chi_M T)_{exp}(i)]^2$). A Curie−Weiss term ($\theta$) was considered in the fit to take into account the possible magnetic interactions between the Ni(II)Gd(III) units through the diamagnetic $[W^{IV}(bipy)(CN)_6]^{2-}$ bridge. Given the large number of parameters involved and in order to avoid overparametrization, the value of g_{Gd} in the fit was fixed to 2.0. The calculated curve matches very well the magnetic data in the whole temperature range explored (see Figure 7). Two alternative fits were perfomed, one fixing $D_{Ni} = 0$ and the other one by assuming that $\theta = 0$. The obtained values were $\theta = -0.42$ K and $D_{Ni} = 12.7\ cm^{-1}$ respectively, the value of J being identical to the previous one. These values of θ and D_{Ni} can be considered as the upper ones for these parameters. However, the agreement between the calculated curves and the experimental data in these fits was not as good as the achieved one when J, D_{Ni}, and θ were the variable parameters. Consequently, we consider the values of the first fit as the best ones.

Let us comment briefly about the magnitude of the best-fit parameters of **1**. The value of the ferromagnetic interaction between the Ni(II) and Gd(III) through the double phenoxo bridge in **1** ($J = +2.57\ cm^{-1}$) is very close to those reported for the discrete herodinuclear complexes $[Ni(CH_3CN)_2(valpn)Gd(NO_3)_3]$ ($J = +2.3\ cm^{-1}$)[24] (**4**) and $[Ni(H_2O)_2(dmvalpn)Gd(NO_3)_3]\cdot CH_3CN$ (H_2dmvalpn = 2,2′-[2,2-dimethyl-1,3-propanediyl-bis(nitrilomethylidyne]bis(6-methoxyphenol) ($J = +3.6\ cm^{-1}$)[30a] (**5**) in agreement with the quasi identical structural parameters of dihenoxo-bridged Ni(II)Gd(III) core

dx.doi.org/10.1021/ic4019794 | Inorg. Chem. 2013, 52, 11627−11637

[values of the Ni···Gd separation and angle at the bridgehead phenoxo-oxygen of 3.49 (**1**), 3.47 (**4**), and 3.52 Å (**5**) and 107.0 (**1**), 106.1 (**2**), 107.2° (**5**)]. Dealing with the value of the zero-field splitting found for the elongated octahedral Ni(II) ion in **1**, it is in agreement with those previously reported for other six-coordinated Ni(II) compounds.[32] Finally, the large Ni···Ni [8.457(1) Å for Ni1···Ni1b], Ni···Gd [8.383(1), 9.683(1) and 9.9.830(1) Å for Ni1b···Gd1a, Ni1b···Gd1 and Ni1···Gd1a] and Gd···Gd [7.951(1) Å for Gd1···Gd1a] distances through the diamagnetic -NC−W^{IV}−CN- pathway accounts for the very weak interdinuclear magnetic interaction found by fit in **1** (θ ca. −0.25 cm^{-1}).

The thermal variation of the $\chi_M T$ product for **3** [χ_M is the magnetic susceptibility per a $Ni^{II}Tb^{III}$ pair] is shown in Figure 8. $\chi_M T$ at 300 K is equal to 12.8 cm^3 mol^{-1} K, a value that is as

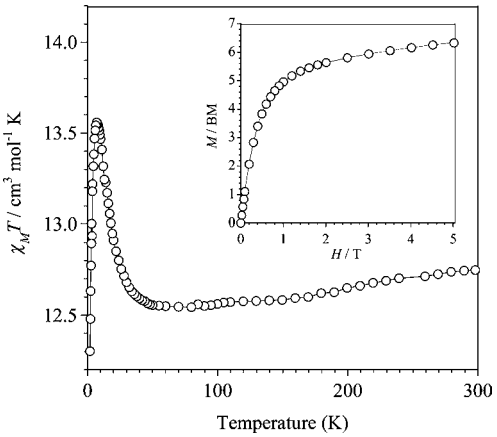

Figure 8. Thermal dependence of $\chi_M T$ (○) for **3**. The inset shows the field dependence of the magnetization at 2.0 K: (○) experimental data; (—) eye-guide line.

expected ($\chi_M T$ = 12.91 cm^3 mol^{-1} K) for a six-coordinated Ni(II) ion ($\chi_M T$ = 1.10 cm^3 mol^{-1} K; S_{Ni} = 1 and g_{Ni} = 2.10) plus a Tb(III) center with a $^7F_6$ low-lying state [$\chi_M T$ = 11.81 cm^3 mol^{-1} K; $4f^8$, J = 6, L = 3, g_J = 3/2, and S = 3] magnetically noninteracting. When the temperature is lowered, $\chi_M T$ decreases smoothly to reach a minimum value of 12.55 cm^3 mol^{-1} K at 60 K, then increases to attain a maximum value of 13.59 at 9.0 K, and finally decreases to 12.30 cm^3 mol^{-1} K at 1.9 K. The profile of the $\chi_M T$ against T curve is strongly suggestive of the occurrence of competitive phenomena. The decrease of $\chi_M T$ in the high-temperature domain is most likely governed by the depopulation of the Tb(III) M_J levels, whereas the increase of $\chi_M T$ after the minimum may be attributed to a ferromagnetic Ni(II)−Tb(III) interaction through the diphenoxo bridge. Finally, the decrease of $\chi_M T$ below 9.0 K is due to magnetic anisotropy effects and/or weak antiferromagnetic interactions between the Ni(II)Tb(III) pairs through the diamagnetic -NC−W^{IV}−CN- bridges. The rapid increase of the magnetization in the region of low applied dc magnetic fields (see inset of Figure 8) supports the occurrence of a ferromagnetic coupling, the reduced value of the M at 5 T (6.50 μ_B) being mainly due to important magnetic anisotropy effects. A quantitative analysis of the magnetic data of **3** is precluded because of the lack of a theoretical model to treat them. Finally, it deserves to be noted that no ac signals were detected for **3** both under zero and nonzero applied dc fields.

The magnetic properties of **2** under the form of $\chi_M T$ versus T plot [$\chi_M T$ is the magnetic susceptibility per Ni(II)Dy(III) unit] are shown in Figure 9. At room temperature, $\chi_M T$ is equal to 15.15 cm^3 mol^{-1} K, a value that is close to the calculated one

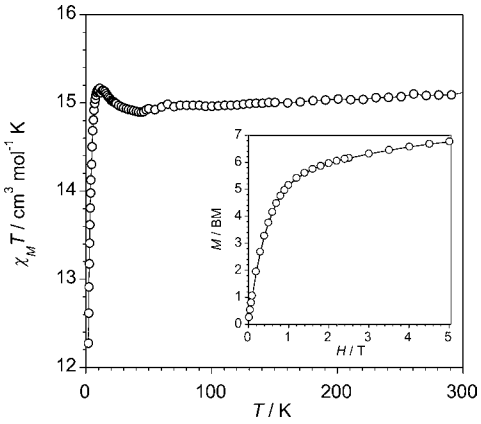

Figure 9. Thermal dependence of $\chi_M T$ (○) for **2**. The inset shows the field dependence of the magnetization at 2.0 K: (○) experimental data; (—) eye-guide line.

of 15.25 cm^3 mol^{-1} K for a six-coordinated Ni(II) ($\chi_M T$ = 1.10 cm^3 mol^{-1} K with S_{Ni} = 1 and g_{Ni} = 2.10) and a Dy(III) [$\chi_M T = (Ng^2_J\beta^2/3k)J(J+1)$ = 14.15 cm^3 mol^{-1} K with J = 15/2 and g_J = 4/3; $4f^9$ electronic configuration and $^6H_{15/2}$ as the low-lying state] pair in the free-ion approximation, considered as magnetically independent centers. The value of $\chi_M T$ decreases slightly with decreasing temperature down to a minimum value of 14.90 cm^3 mol^{-1} K at ca. 45 K and then increases at lower temperatures, reaching a maximum value of 15.20 cm^3 mol^{-1} K at 9.0. Below this temperature, the $\chi_M T$ value drops abruptly to 12.25 cm^3 mol^{-1} K at 1.9 K. The slight decrease of $\chi_M T$ in the high temperature regime is due to the depopulation of the M_J sublevels of the Dy(III) ion which arise from the splitting of the $^6H_{15/2}$ ground term by the ligand field and whose width is about 100 cm^{-1}. The increase of $\chi_M T$ after the mimimum is most likely due to a ferromagnetic interaction between the Ni(II) and the Dy(III) ions through the diphenoxo bridge whereas the decrease of $\chi_M T$ below 9.0 K is probably associated to the presence of magnetic anisotropy and/or weak antiferromagnetic interactions between the Ni(II)Dy(II) pairs through the diamagnetic -NC−W^{IV}−CN- bridging pathway. The ferromagnetic interaction between the Ni(II) and Dy(III) through the diphenoxo bridge in **2** is supported in view of the magneto-structural studies carried out for other systems containing this bridging pathway.[24,30f,g] However, its evaluation though a quantitative analysis of the magnetic susceptibility data is precluded because of the occurrence of spin−orbit coupling and crystal field effects.

The field dependence of the magnetization at 2.0 K for **2** (see inset of Figure 9) reveals a relatively slow increase of the magnetization at low fields and then a linear increase without saturation; the value of M at 5 T (the maximum value in our device) is ca. 6.8 μ_B. The linear high-field variation of M suggests the occurrence of a significant magnetic anisotropy and/or low-lying exciting states which are partially populated. These states are in agreement with the weak magnetic interactions expected for mixed 3d-4f systems.

Alternating current (ac) magnetic susceptibility measurements were performed on **2** in order to investigate the possible slow relaxation of the magnetization. In fact, this compound exhibits frequency dependence of the in-phase (χ_M') [see

dx.doi.org/10.1021/ic4019794 | Inorg. Chem. 2013, 52, 11627−11637

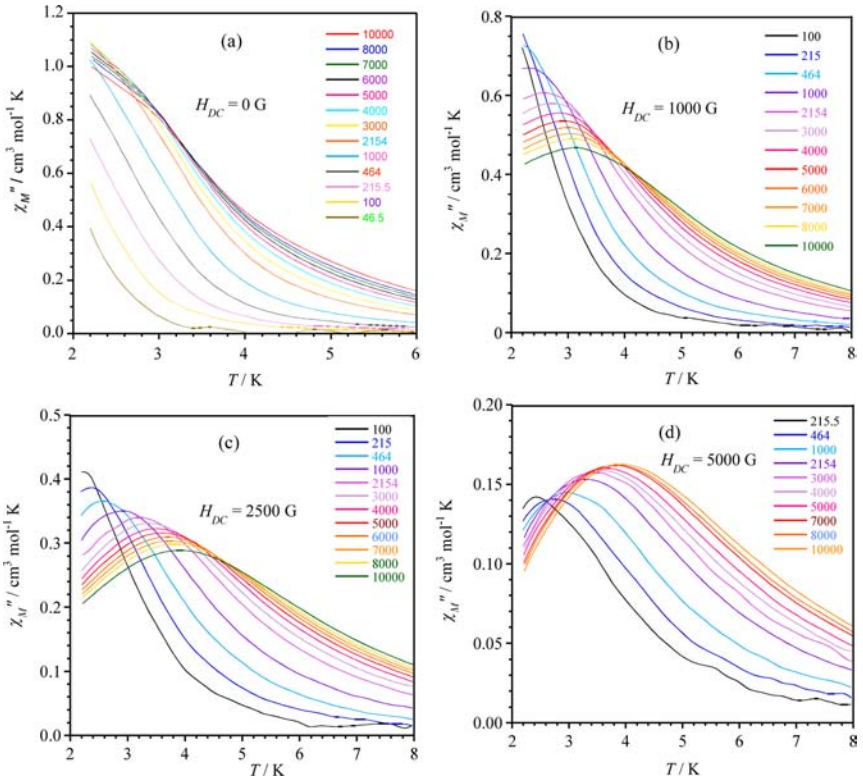

Figure 10. Frequency and temperature dependence of the out-of-phase magnetic susceptibility under external applied dc magnetic fields 0 (a), 1000 (b), 2500 (c), and 5000 G (d) in a ± 4 G oscillating field and in the frequency range 46.5−10000 Hz for **2**.

Figure S6] and out-of-phase (χ_M'') [Figure 10] signals and, therefore, slow relaxation of magnetization typical for an SMM. No maxima of χ_M'' are observed above 2.20 K in the frequency range explored under a dc field H_{dc} = 0 G [Figure 10(a)]. However, maxima of χ_M'' appear at T > 2.20 K under applied dc fields of 1000, 2500, and 5000 G (Figure 10b−d), with their positions being shifted to higher temperatures with increasing field. The data obtained for each nonzero dc field were fit to the Arrhenius equation $\tau = \tau_0 \exp(E^{\#}/kT)$, with the values of τ_0 (preexponential factor) and E_a (energy barrier) covering the ranges 2.3−7.0 × 10^{-8} s and 12.8−18.4 cm^{-1} (see Figure S7 and Table 5) and are very close to those found for a

Table 5. Values of the Preexponential Factor (τ_0) and Activation Energy ($E^{\#}$) for 2

H/G	$\tau_0 \times 10^8$/s	$E^{\#}$/cm^{-1}
5000	2.3	18.4
2500	5.7	15.9
1000	7.0	12.8
0	≈50	≈8

{Ni(valpn)Dy} dimer or a double chain constructed from {Ni(valpn)Dy} nodes.[21i] Although no maxima of χ_M'' are observed for **2** above 2.2 K in the lack of an applied dc magnetic field, a rough evaluation of $E^{\#}$ and τ_0 can be done from the $\ln(\chi_M''/\chi_M')$ versus $1/T$ plot at a given frequency of the alternating current (ac) field and by assuming only a single relaxation time (Figure S8). This methodology has been applied successfully in other examples of SMMs.[33] The values so obtained are ca. 50 × 10^{-8} s and 8.0 cm^{-1} for τ_0 and $E^{\#}$, respectively. These values are in agreement with those previously reported for similar 3d/4f SMM systems.[30g,34] The fact that the χ_M'' vs χ_M' plots (Cole−Cole plots)[35] in the frequency range 100−10000 Hz at different temperatures and dc field values for **2** give incomplete semicircles (Figure S9) precludes their analysis.

CONCLUDING REMARKS

In summary, the three isomorphous polynuclear complexes, $[Ni^{II}(valpn)Ln^{III}(NO_3)(H_2O)(\mu\text{-}NC)_4W^{IV}(bipy)(CN)_2]_n$ presented in this work show a unique 2D porous framework with binuclear nodes, $[Ni(valpn)Ln(O_2NO)_3]$, which are interconnected by heteroleptic diamagnetic $[W^{IV}(bipy)(CN)_6]^{2-}$ spacers. The reduction of the starting precursor $[W^{V}(bipy)(CN)_6]^{-}$ to $[W^{IV}(bipy)(CN)_6]^{2-}$ during the reaction process caused the volume to increase allowing the highest denticity (tetradentate) found to date for a heteroleptic cyanido-complex of tungsten. Moreover, the Dy^{III} derivative exhibits slow relaxation of the magnetization due to SMM behavior of the $\{Ni^{II}Dy^{III}\}$ diphenoxo-bridged moiety, which is further connected by the heteroleptic $[W^{IV}(bipy)(CN)_6]^{2-}$ linkers to afford a neutral 2D coordinative assembly of SMMs.

ASSOCIATED CONTENT

Supporting Information

Hydrogen bonds [Tables S1 (**1**)], structural drawings (Figures S1−S5), and magnetic plots (Figures S6−S9). This material is available free of charge via the Internet at http://pubs.acs.org. CCDC 953098 (**1**), 953097 (**2**) and 953096 (**3**) contain the X-ray crystallographic data in cif files.

AUTHOR INFORMATION

Corresponding Authors

*(M.A.) E-mail: marius.andruh@dnt.ro.
*(M.J.) E-mail: miguel.julve@uv.es.

Notes

The authors declare no competing financial interest.

■ ACKNOWLEDGMENTS

Financial support from the Romanian Ministry of Education CNCS-UEFISCDI (Projects PN-II-RUPD-2012-3-0177, PNII-ID-PCCE-2011-2-0050), the Ministerio Español de Ciencia e Innovación (CTQ2010-15364), and the Generalitat Valenciana (ISIC/2012/002) is gratefully acknowledged.

■ REFERENCES

(1) Verdaguer, M.; Bleuzen, A.; Marvaud, V.; Vaissermann, J.; Seuleiman, M.; Desplanches, C.; Scuiller, A.; Train, C.; Garde, R.; Gelly, G.; Lomenech, C.; Rosenman, I.; Veillet, P.; Cartier, C.; Villain, F. *Coord. Chem. Rev.* **1999**, *190*−*192*, 1023.

(2) Ohba, M.; Okawa, H. *Coord. Chem. Rev.* **2000**, *198*, 313.

(3) Kou, H.-Z.; Zhou, B. C.; Gao, S.; Wang, R.-J. *Angew. Chem., Int. Ed. Engl.* **2003**, 3288.

(4) Herrera, J. M.; Bleuzen, A.; Dromzée, Y.; Julve, M.; Lloret, F.; Verdaguer, M. *Inorg. Chem.* **2003**, *42*, 7052.

(5) Tanase, S.; Reedijk, J. *Coord, Chem.. Rev.* **2006**, *250*, 2501.

(6) (a) Sieklucka, B.; Podgajny, R.; Przychodzeń, P.; Korzeniak, T. *Coord. Chem. Rev.* **2005**, *249*, 2203. (b) Przychodzeń, P.; Korzeniak, T.; Podgajny, R.; Sieklucka, B. *Coord. Chem. Rev.* **2006**, *250*, 2234. (c) Sieklucka, B.; Podgajny, R.; Korzeniak, T.; Nowicka, B.; Pinkowicz, D.; Kozieł, M. *Eur. J. Inorg. Chem.* **2011**, 305.

(7) (a) Figuerola, A.; Ribas, J.; Llunell, M.; Casanova, D.; Maestro, M.; Alvarez, S.; Díaz, C. *Inorg. Chem.* **2005**, *44*, 6939. (b) Figuerola, A.; Ribas, J.; Casanova, D.; Maestro, M.; Alvarez, S.; Díaz, C. *Inorg. Chem.* **2005**, *44*, 6949. (c) Estrader, M.; Ribas, J.; Tangoulis, V.; Solans, X.; Font-Bardía, M.; Maestro, M.; Díaz, C. *Inorg. Chem.* **2006**, *45*, 8239.

(8) (a) Marvaud, V.; Decroix, C.; Scuiller, A.; Guyard, D.; Vaissermann, J.; Gonnet, F.; Verdaguer, M. *Chem.—Eur. J.* **2003**, *9*, 1678. (b) Marvaud, V.; Decroix, C.; Scuiller, A.; Tuyèras, F.; Guyard-Duhayon, C.; Vaissermann, J.; Marrot, J.; Gonnet, F.; Verdaguer, M. *Chem.—Eur. J.* **2003**, *9*, 1692. (c) Tuyèras, F.; Scuiller, A.; Duhayon, C.; Hernández-Molina, M.; Fabrizi di Biani, F.; Verdaguer, M.; Mallah, T.; Wernsdorfer, W.; Marvaud, V. *Inorg. Chim. Acta* **2008**, *361*, 3505.

(9) (a) Shatruk, M.; Avendaño, C.; Dunbar, K. R. *Prog. Inorg. Chem.* **2009**, *47*, 832. (b) Wang, X.-Y.; Avendaño, C.; Dunbar, K. R. *Chem. Soc. Rev.* **2011**, *40*, 3213.

(10) (a) Visinescu, D.; Madalan, A. M.; Andruh, M.; Duhayon, C.; Sutter, J.-P.; Ungur, L.; Van den Heuvel, W.; Chibotaru, L. F. *Chem.—Eur. J.* **2009**, *15*, 11808. (b) Maxim, C.; Sorace, L.; Khuntia, P.; Madalan, A. M.; Kravtsov, V.; Lascialfari, A.; Caneschi, A.; Journaux, Y.; Andruh, M. *Dalton Trans.* **2010**, *39*, 4838. (c) Stoian, S. A.; Paraschiv, C.; Kiritsakas, N.; Lloret, F.; Münck, E.; Bominaar, E. L.; Andruh, M. *Inorg. Chem.* **2010**, *49*, 3387. (d) Gheorghe, R.; Madalan, A. M.; Costes, J.-P.; Wernsdorfer, W.; Andruh, M. *Dalton Trans.* **2010**, *39*, 4734. (e) Visinescu, D.; Jeon, I.-R.; Madalan, A. M.; Alexandru, M.-G.; Jurca, B.; Mathonière, C.; Clérac, R.; Andruh, M. *Dalton Trans.* **2012**, *41*, 13578.

(11) (a) Lescouëzec, R.; Toma, L. M.; Vaissermann, J.; Verdaguer, M.; Delgado, F. S.; Ruiz-Pérez, C.; Lloret, F.; Julve, M. *Coord. Chem. Rev.* **2005**, *249*, 2691. (b) Visinescu, D.; Toma, L. M.; Lloret, F.; Fabelo, O.; Ruiz-Pérez, C.; Julve, M. *Dalton Trans.* **2008**, 4103. (c) Visinescu, D.; Toma, L. M.; Cano, J.; Fabelo, O.; Ruiz-Pérez, C.; Labrador, A.; Lloret, F.; Julve, M. *Dalton Trans.* **2010**, *39*, 5028. (d) Visinescu, D.; Fabelo, O.; Ruiz-Pérez, C.; Lloret, F.; Julve, M. *CrystEngComm.* **2010**, *12*, 2454. (e) Toma, L. M.; Pasán, J.; Ruiz-Pérez, C.; Lloret, F.; Julve, M. *Dalton Trans.* **2012**, *41*, 13716. (f) Toma, L. M.; Ruiz-Pérez, C.; Pasán, J.; Wernsdorfer, W.; Lloret, F.; Julve, M. *J. Am. Chem. Soc.* **2012**, *134*, 15265. (g) Toma, L. M.; Ruiz-Pérez, C.; Lloret, F.; Julve, M. *Inorg. Chem.* **2012**, *51*, 1216. (h) Wang, S.; Ding, X.-H.; Li, Y.-H.; Huang, W. *Coord. Chem. Rev.* **2012**, *256*, 439.

(12) Wang, H.; Zhang, L.-F.; Ni, Z.-H.; Zhong, W.-F.; Tian, L.-J.; Jiang, J. *Cryst. Growth Des.* **2010**, *10*, 4231.

(13) (a) Kim, J. I.; Yoon, J. H.; Kwak, H. Y.; Koh, E. K.; Hong, C. S. *Eur. J. Inorg. Chem.* **2008**, 2756. (b) Choi, S. W.; Kwak, H. Y.; Yoon, J. H.; Kim, H.; Koh, E. K.; Hong, C. S. *Inorg. Chem.* **2008**, *47*, 10214. (c) Choi, S. W.; Ryu, D. W.; Lee, J. W.; Yoon, J. H.; Kim, H. C.; Lee, H.; Cho, B. K.; Hong, C. S. *Inorg. Chem.* **2009**, *48*, 9066. (d) Alexandru, M.-G.; Visinescu, D.; Madalan, A. M.; Lloret, F.; Julve, M.; Andruh, M. *Inorg. Chem.* **2012**, *51*, 4906. (e) Korzeniak, T.; Nowicka, B.; Stadnicka, K.; Nitek, W.; Majcher, A. M.; Sieklucka, B. *Polyhedron* **2013**, *52*, 442.

(14) Szklarzewicz, J.; Podgajny, R.; Lewinski, K.; Sieklucka, B. *CrystEngComm* **2002**, *4*, 199.

(15) (a) Visinescu, D.; Toma, L. M.; Fabelo, O.; Ruiz-Pérez, C.; Lloret, F.; Julve, M. *Inorg. Chem.* **2013**, *52*, 1525. (b) Xiang, H.; Wang, S. J.; Jiang, L.; Feng, X. L.; Lu, T. B. *Eur. J. Inorg. Chem.* **2009**, 2074.

(16) (a) Zhang, Y. Z.; Wang, Z. M.; Gao, S. *Inorg. Chem.* **2006**, *45*, 10404. (b) Zhang, Y. Z.; Wang, Z. M.; Gao, S. *Inorg. Chem.* **2006**, *45*, 5447. (c) Zhang, Y. Z.; Gao, S.; Sun, H. L.; Su, G.; Wang, Z. M.; Zhang, S. W. *Chem. Commun.* **2004**, 1906.

(17) (a) Yeung, W. F.; Lau, P. H.; Lau, T. C.; Wei, H. Y.; Sun, H. L.; Gao, S.; Chen, Z. D.; Wong, W. T. *Inorg. Chem.* **2005**, *44*, 6579. (b) Yeung, W. F.; Lau, T. C.; Wang, X. Y.; Gao, S.; Szeto, L.; Wong, W. T. *Inorg. Chem.* **2006**, *45*, 6756. (c) Toma, L. M.; Toma, L. D.; Delgado, F. S.; Ruiz-Pérez, C.; Sletten, J.; Cano, J.; Clemente-Juan, J. M.; Lloret, F.; Julve, M. *Coord. Chem. Rev.* **2006**, *250*, 2176. (d) Yeung, W. F.; Man, W. L.; Wong, W. T.; Lau, T. C.; Gao, S. *Angew. Chem., Int. Ed.* **2001**, *40*, 3031.

(18) (a) Herrera, J. M.; Baca, S. G.; Adams, H.; Ward, M. D. *Polyhedron* **2006**, *25*, 869. (b) Davies, G. M.; Pope, S. J. A.; Adams, H.; Faulkner, S.; Ward, M. D. *Inorg. Chem.* **2005**, *44*, 4656.

(19) (a) Mannini, M.; Pineider, F.; Sainctavit, Ph.; Danieli, C.; Otero, E.; Sciancalepore, C.; Talarico, A. M.; Arrio, M.-A.; Cornia, A.; Gatteschi, D.; Sessoli, R. *Nat. Mater.* **2009**, *8*, 194. (b) Mannini, M.; Pineider, F.; Danieli, C.; Totti, F.; Sorace, L.; Sainctavit, Ph.; Arrio, M.-A.; Otero, E.; Joly, L.; Cezar, J. C.; Cornia, A.; Sessoli, R. *Nature* **2010**, *468*, 417. (c) Cornia, A.; Mannini, M.; Sainctavit, Ph.; Sessoli, R. *Chem. Soc. Rev.* **2011**, *40*, 3076.

(20) (a) Jeon, I.-R.; Clérac, R. *Dalton Trans.* **2012**, *41*, 9569. (b) Lecren, L.; Wernsdorfer, W.; Li, Y.-G.; Vindigni, A.; Miyasaka, H.; Clérac, R. *J. Am. Chem. Soc.* **2007**, *129*, 5045. (c) Inglis, R.; Jones, L. F.; Mason, K.; Collins, A.; Moggach, S. A.; Parson, S.; Perlepes, S. P.; Wernsdorfer, W.; Brechin, E. K. *Chem.—Eur. J.* **2008**, *14*, 9117. (d) Inglis, R.; Giannis, A.; Papaefstathiou, S.; Wernsdorfer, W.; Brechin, E. K. *Aust. J. Chem.* **2009**, *62*, 1108.

(21) (a) Miyasaka, H.; Nakata, K.; Sugiura, K.-I.; Yamashita, M.; Clérac, R. *Angew. Chem., Int. Ed.* **2004**, *43*, 707. (b) Jeon, I.-R.; Ababei, R.; Lecren, L.; Li, Y.-G.; Wernsdorfer, W.; Roubeau, O.; C. Mathonière, C.; Clérac, R. *Dalton Trans.* **2010**, *39*, 4744. (c) Novitchi, G.; Pilet, G.; Ungur, L.; Moshchalkov, V. V.; Wernsdorfer, W.; Chibotaru, L. F.; Luneau, D.; Powell, A. K. *Chem. Sci.* **2012**, *3*, 1169. (d) Lecren, L.; Roubeau, O.; Li, Y.-G.; Le Golf, X.; Miyasaka, H.; Richard, F.; Wernsdorfer, W.; Coulon, C.; Clérac, R. *Dalton Trans.* **2008**, 755. (e) Moushi, E. E.; Stamatatos, T. C.; Wernsdorfer, W.; Nastopoulos, V.; Christou, G.; Tasiopoulos, A. J. *Angew. Chem., Int. Ed.* **2006**, *45*, 7722. (f) Tsai, H.-L.; Yang, C.-I; Wernsdorfer, W.; Huang, S.-H.; Jhan, S.-Y.; Liu, M.-H.; Lee, G.-H. *Inorg. Chem.* **2012**, *51*, 13171. (g) Miyasaka, H.; Nakata, K.; Lecren, L.; Coulon, C.; Nakazawa, Y.; Fujisaki, T.; Sugiura, K.-I.; Yamashita, M.; Clérac, R. *J. Am. Chem. Soc.* **2006**, *128*, 3770. (h) Katsenis, A. D.; Inglis, R.; Prescimone, A.; Brechin, E. K.; Papaefstathiou, G. S. *CrystEngComm* **2012**, *14*, 1216. (i) Pasatoiu, T. D.; Etienne, M.; Madalan, A. M.; Andruh, M.; Sessoli, R. *Dalton Trans.* **2010**, *39*, 4802. (j) Kachi-Terajima, C.; Mori, E.; Eiba, T.; Saito, T.; Kanadani, C.; Kitazawa, T.; Miyasaka, H. *Chem. Lett.* **2010**, *39*, 94. (k) Liu, Y.; Chen, Z.; Ren, J.; Zhao, X.-Q.; Cheng, P.; Zhao, B. *Inorg. Chem.* **2012**, *51*, 7433.

(22) (a) Vigato, P. A.; Tamburini, S. *Coord. Chem. Rev.* **2004**, *248*, 1717. (b) Robson, R. *Dalton Trans.* **2008**, 5113.

(23) (a) Andruh, M. *Chem. Commun.* **2011**, *47*, 3025. (b) Andruh, M. *Chem. Commun.* **2007**, 2565.

(24) Pasatoiu, T. D.; Sutter, J.-P.; Madalan, A. M.; Chiboub Fellah, F. Z.; Duhayon, C.; Andruh, M. *Inorg. Chem.* **2011**, *50*, 5980.
(25) (a) Stawski, T.; Szklarzewicz, J.; Lewinski, K. *Trans. Met. Chem.* **2006**, *31*, 353. (b) Szklarzewicz, J. *Inorg. Chim. Acta* **1993**, *205*, 85.
(26) *CrysAlis RED*, Version 1.171.34.76; Oxford Diffraction Ltd.: Yarnton, U.K., 2003.
(27) Sheldrick, G. M. *Acta Crystallogr.* **2008**, *A64*, 112.
(28) (a) Wang, Z.-X.; Zhang, P.; Shen, X.-F.; Song, Y.; You, X.-Z.; Hashimoto, K. *Cryst. Growth Des.* **2006**, *6*, 2457. (b) Podgajny, R.; Chmel, N. P.; Bałanda, M.; Tracz, P.; Gaweł, B.; Zajac, D.; Sikora, M.; Kapusta, C.; Łasocha, W.; Wasiutynski, T.; Sieklucka, B. *J. Mater. Chem.* **2007**, *17*, 3308. (c) Wang, Z.-X.; Wei, J.; Li, Y.-Z.; Guo, J.-S.; Song, Y. *J. Mol. Str.* **2008**, *875*, 198. (d) Wang, Y.; Wang, T.-W.; Xiao, H.-P.; Li, Y.-Z.; Song, Y.; You, X.-Z. *Chem.—Eur. J.* **2009**, *15*, 7648. (e) Qian, J.; Yoshikawa, H.; Zhang, J.; Zhao, H.; Awaga, K.; Zhang, C. *Cryst. Growth Des.* **2009**, *9*, 5351. (f) Qian, J.; Zhao, H.; Wei, H.; Li, J.; Zhang, J.; Yoshikawa, H.; Awaga, K.; Zhang, C. *CrystEngComm* **2011**, *13*, 517.
(29) Ribas, J. *Coordination Chemistry*; Wiley-VCH: Weinheim, Germany, 2008; p 33.
(30) (a) Costes, J.-P.; Dahan, F.; Dupuis, A.; Laurent, J.-P. *Inorg. Chem.* **1997**, *36*, 4284. (b) Yamaguchi, T.; Sunatsuki, Y.; Kojima, M.; Akashi, H.; Tsuchimoto, M.; Re, N.; Osa, S.; Matsumoto, N. *Chem. Commun.* **2004**, 1048. (c) Costes, J.-P.; Yamaguchi, T.; Kojima, M.; Vendier, L. *Inorg. Chem.* **2009**, *48*, 5555. (d) Wang, J.-H.; Yan, P.-F.; Li, G.-M.; Zhang, J.-W.; Chen, P.; Suda, M.; Einaga, Y. *Inorg. Chim. Acta* **2010**, *363*, 3706. (e) Singh, S. K.; Tibrewal, N. K.; Rajaraman, G. *Dalton Trans.* **2011**, *40*, 10897. (f) Colacio, E.; Ruiz-Sánchez, J.; White, F. J.; Brechin, E. K. *Inorg. Chem.* **2011**, *50*, 7268. (g) Palacios, M. A.; Mota, A. J.; Ruiz, J.; Hänninen, M. M.; Sillanpää, R.; Colacio, E. *Inorg. Chem.* **2012**, *51*, 7010. (h) Sakamoto, S.; Suguru, Y.; Hagiwara, H.; Matsumoto, N.; Sunatsuki, Y.; Re, N. *Inorg. Chem. Commun.* **2012**, *26*, 20.
(31) Cano, J. *VMPAG* package; University of València: Spain, 2003.
(32) Boca, R. *Coord. Chem. Rev.* **2004**, *248*, 757.
(33) (a) Ferrando-Soria, J.; Cangussu, D.; Eslava, M.; Journaux, Y.; Lescouëzec, R.; Julve, M.; Lloret, J.; Pasán, J.; Ruiz-Pérez, C.; Lhotel, E.; Paulsen, C.; Pardo, E. *Chem.—Eur. J.* **2011**, *17*, 12482. (b) Martínez-Lillo, J.; Mastropietro, T. F.; De Munno, G.; Lloret, F.; Julve, M.; Faus, J. *Inorg. Chem.* **2011**, *50*, 5731.
(34) Chandrasekhar, V.; Pandian, B. M.; Boomishankar, R.; Steiner, A.; Vittal, J. J.; Houri, A.; Clérac, R. *Inorg. Chem.* **2008**, *47*, 4918 and references therein.
(35) Cole, K. S.; Cole, R. H. *J. Chem. Phys.* **1941**, *9*, 341.